Available online at www.sciencedirect.com
SCIENCE DIRECT®
Biochemical Pharmacology 68 (2004) 513–521
Biochemical Pharmacology
www.elsevier.com/locate/biochempharm

Acetaminophen alters microsomal ryanodine Ca^{2+} channel in HepG2 cells overexpressing CYP2E1

Adam Holownia*, Jan J. Braszko

Department of Clinical Pharmacology, Medical Academy of Bialystok, Waszyngtona 15A, 15-274 Bialystok, Poland

Received 17 February 2004; accepted 13 April 2004

Abstract

Acetaminophen hepatotoxicity is mediated by an initial metabolic activation and covalent binding of drug metabolites to liver proteins. Acetaminophen metabolites have been shown to affect rat liver microsomal Ca^{2+} stores, but the mechanism is not well understood. The aim of the current work was to find out if the metabolism of acetaminophen by CYP2E1 affects ryanodine-sensitive Ca^{2+} stores in the endoplasmic reticulum of transduced HepG2 cells. Five millimoles acetaminophen decreased proliferation of CYP2E1-overexpressing HepG2 cells, increased cytosolic Ca^{2+} levels and produced significant cytotoxicity, while only little, mostly anti-proliferative effects were found in HepG2 cells lacking CYP2E1. CYP2E1 inhibitor-4-methylpyrazole decreased drug cytotoxicity in transduced cells and normalized elevated Ca^{2+} levels. Acetaminophen cytotoxicity was significantly higher in CYP2E1 expressing cells with depleted glutathione. In the cells engineered to overexpress CYP2E1, an increased [^{3}H]ryanodine affinity (by 45%) and increased ligand maximal binding to ryanodine receptors (by 64%) was observed, most probably due to increased association rate of [^{3}H]ryanodine. Ca^{2+} loading was decreased by about 53% in microsomal fractions isolated from transduced cells treated with acetaminophen and by 92% in glutathione depleted transfected cells treated with the drug. Ca^{2+}/Mg^{2+}-ATPase activity was unchanged in all microsomal fractions. Such effects were not observed in cells lacking CYP2E1. Our results confirm significant role of CYP2E1 in metabolic activation of acetaminophen and indicate that ryanodine receptors located in the liver endoplasmic reticulum are sensitive targets for acetaminophen metabolites.

Keywords: Acetaminophen; Calcium; CYP2E1; Microsomal ryanodine channel

Acetaminophen (APAP; paracetamol; *N*-acetyl-*p*-aminophenol) is a relatively safe, widely used analgesic, but APAP overdose may cause centrilobular hepatic necrosis [1]. The hepatotoxicity of the drug is believed to result from its CYP2E1, CYP3A4 and CYP1A2-dependent activation to reactive *N*-acetyl-*p*-aminobenzoquinone imine (NAPQI) [2–5]. Experiments with ^{14}C-acetaminophen and immunochemical quantification of 3-(cystein-*S*-yl)acetaminophen protein adducts have shown the presence of drug metabolite adducts in cytosolic, mitochondrial and microsomal fractions of the liver cells [6–8]. NAPQI can produce a dose-dependent depletion of intracellular glutathione and protein thiols [3,9–11]. There is substantial evidence that the acetaminophen-dependent alteration of the cellular thiols is followed by perturbations of the calcium homeostasis [12–14]. In in vitro experiments, it was shown, that NAPQI released Ca^{2+} from intact mitochondria [12,15].

Increased cytosolic Ca^{2+} levels may also result from activation of the calcium channels of the endoplasmic reticulum, which are responsible for mobilization of stored calcium. It was reported, that NAPQI induced Ca^{2+} release from rat liver microsomes without affecting the microsomal Ca^{2+}/Mg^{2+}-ATPase; the releasing process, however, was paralleled by a pronounced modulation of the ryanodine binding to the microsomal membranes [16]. The skeletal and cardiac isoforms of ryanodine receptors (RyRs) have cysteine sufhydryls whose alkylation or conversion to disulfide(s) opens the channels for Ca^{2+} [17–19] and it is possible that the liver RyR may share the same properties.

Abbreviations: APIII, antipyrylazo III; APAP, *N*-acetyl-*p*-aminophenol; BSO, buthionine sulfoximine; C34 cells, HepG2 cells transfected with empty vector; E47 cells, HepG2 cells transfected with CYP2E1; MP, 4-methylpyrazole; NAPQI, *N*-acetyl-*p*-aminobenzoquinone imine; PI, propidium iodide; RyR, ryanodine receptor

* Corresponding author. Tel.: +48-85-7450-649; fax: +48-85-7421-838.
E-mail address: Holow_sinai@hotmail.com (A. Holownia).

0006-2952/$ – see front matter © 2004 Elsevier Inc. All rights reserved.
doi:10.1016/j.bcp.2004.04.007

In the present study, we evaluated whether the metabolism of APAP affects ryanodine-sensitive calcium stores in HepG2 cells (C34 cells) and in HepG2 cells, which overexpress CYP2E1 (E47 cells).

1. Experimental procedures

1.1. Cells and reagents

The human hepatoblastoma cell subline-HepG2 stably transfected with human CYP2E1 (E47 cells) and HepG2 cells transfected with an empty vector (C34 cells) used in this study were kindly provided by Dr Arthur Cederbaum of the Department of Pharmacology and Biological Chemistry, Mount Sinai School of Medicine. Cells were grown in minimal essential medium supplemented with 10% Fetal Bovine Serum, penicillin (100 U/ml) and streptomycin (100 μg/ml). The cell cultures were incubated at 37 °C in a humidified atmosphere of 5% CO_2. For maintaining CYP2E1 expression, the medium was additionally supplemented with G418-sulfate (200 μg/ml), the antibiotic used for the selection process.

[^{3}H]ryanodine (61 Ci/mmol) was from New England Nuclear; Pluronic F-127 and Fura-2AM were obtained from Molecular Probes (Molecular Probes Inc). All other reagents were purchased from Sigma Chemical Co.

1.2. CYP2E1 activity

The activity of CYP2E1 in E47 cells determined by following the oxidation of *p*-nitrophenol was 230 pmol/(min mg) microsomal protein. No such activity was detected in C34 cells.

1.3. APAP treatment

C34 and E47 cells were grown in Coulter flasks in minimal essential medium supplemented with 5% (v/v) fetal bovine serum and antibiotics. Forty eight hours prior to APAP treatment the cells were trypsinized, split and optimally divided for the particular assays; 24 h before APAP treatment, the attached cells were switched to an antibiotics-free media. The cells were grown in the presence of 5 mM APAP for 48 h. APAP cytotoxicity was assessed also in cells with depleted glutathione (24 h pretreatment with 100 μM buthionine sulfoximine (BSO), [6,20] and in the presence of 5 mM 4-methylpyrazole (MP), a CYP2E1 inhibitor.

1.4. Determination of cell viability

APAP cytotoxicity was estimated by flow cytometry [21] after DNA staining with propidium iodide (PI; 50 μg/ml, 30 min) in Tris buffer (100 mM; pH 7.5), containing potassium cyanide (0.1%), NP-40 (0.01%), RNAse (40 μg/ml; Type III-A, 4 KU/ml) and NaN_3 (0.1%). Cellular DNA profiles and cell cycle analysis were performed on an aligned Coulter epics profile flow cytometer equipped with an argon laser operating at 488 nm with adjusted forward angle- and side light-scatter. PI fluorescence was measured in 10,000 cells within a spectral range from 200 to 800 nm with appropriate dichroic splitting and bandpass filters. DNA histograms were analyzed by DNA analysis software (MultiCycle, Phoenix Flow Systems Inc). The cells were quantified by their relative distribution in the hypodiploid (early GO/G1 zone of the DNA fluorescence histograms), diploid (G0/G1 zone-pre-DNA synthesis/resting), S-phase (DNA synthesis), and G2/M (post-DNA synthesis/mitosis) phases of the cell cycle.

1.5. Measurement of intracellular Ca^{2+}

Cells were loaded with Fura-2 acetoxymethylester (Fura-2AM; 5 μM; stock solution in DMSO) in a phosphate buffer (1 mM; pH 7.4) containing NaCl (139 mM), KCl (3 mM), $MgCl_2$ (10 mM), HEPES (10 mM), albumin (0.2%), sucrose (15 mM), glucose (5 mM) and Pluronic F-127 (0.02%), [22]. After incubation for 30 min (20 °C), the cells were washed twice with a Fura-2-free incubation buffer and the fluorescence was measured on a Perkin-Elmer fluorimeter using an emission wavelength of 476 nm and excitation wavelength of 340 nm. The cellular Ca^{2+} concentration was quantified using standard Ca-EGTA solutions [23].

1.6. Isolation of microsomal membranes

Scraped cells were briefly sonicated on ice and microsomal membranes were isolated by differential centrifugation [24].

1.7. Measurement of Ca^{2+} transport

Ca^{2+} uptake and release by microsomes isolated from control and APAP-treated cells was monitored using a Perkin-Elmer Lambda EZ201 spectrophotometer and differential absorption changes of antipyrylazo III (AP III) at 710 and 790 nm (16). In a typical experiment, uptake and release of Ca^{2+} was measured in microsomal suspensions (0.5 mg protein/ml) in 0.1 M phosphate buffer (pH 7.0), containing KCl (0.1 M), HEPES (20 mM), Mg^{2+} (0.5 mM), ATP (0.5 mM) and an ATP-regenerating system consisting of creatine phosphokinase (30 U/ml) and creatine phosphate (8 mM). Experiments were initiated by the addition of $CaCl_2$ (final Ca^{2+} concentration of 0.1 mM) and changes in absorbance of AP III were plotted against time.

The "Ca^{2+}/Mg^{2+}-ATPase activity" was determined by measuring the accumulation of inorganic phosphate during the hydrolysis of ATP [25]. Microsomes (0.025 mg/ml) were incubated for 20 min at 37 °C in HEPES (0.05 M, pH

7.0), containing ATP (1 mM), ouabain (0.2 mM), $CaCl_2$ (0.06 mM), alamethacin (0.001 mg/ml) and $MgCl_2$ (0.5 mM). The reaction was stopped by addition of 0.3 ml of 20% (w/v) trichloroacetic acid and, after centrifugation (3 min × 5000 × *g*), an aliquot of 0.1 ml was transferred into a solution of 0.034% malachite green (0.8 ml, in 1 M HCl). The color development was fixed by addition of 0.1 ml of 1% ammonium molybdate and absorbance was determined at 640 nm.

[^{3}H]ryanodine binding kinetics: association rate of [^{3}H]ryanodine (specific activity 61.0 Ci/mmol) to RyRs was determined with [^{3}H]ryanodine and microsomes from E47 cells or E47 cells treated with 5 mM APAP for 48 h. Ligand association was measured using 15 nM [^{3}H]ryanodine in 20 mM Hepes buffer (pH 7.1) containing of 250 mM KCl, 15 mM NaCl and 1 mM EGTA. Ligand dissociation from the equilibrium complex was measured after 1:100 dilution of equilibrated samples with incubation buffer. Association and dissociation rate constants were calculated with Origin 6.1 software (Microcal Inc.) using non-linear regression.

[^{3}H]ryanodine equilibrium binding was determined using 5 nM [^{3}H]ryanodine and 1-500 nM [^{3}H]ryanodine in 20 mM Hepes buffer (pH 7,1) containing of 250 mM KCl, 15 mM NaCl and 1 mM EGTA to determine non-specific binding [26]. Samples were incubated in the same incubation buffer as in triplicate for 180 min in the dark at 37 °C, vacuum filtrated onto polyethyleneimine-treated Whatman GF/B glass fiber filters, washed twice with 4 ml of ice-cold wash buffer (5 mM Tris–HCl, pH 7.0, 0.5 M KCl, 250 μM $CaCl_2$) and once with ice-cold 70% ethyl alcohol. The radioactivity remaining on the filters was quantified in a scintillation counter (Beckman 6500). The binding data were fitted to a one-site model with Origin 6.1 software, using non-linear regression and Scatchard–Rosenthal analysis. The affinity constant of the [^{3}H]ryanodine–RyR complex (k_d) and the maximal density of binding sites (B_{max}) values were obtained from saturation binding curves.

1.8. Data analysis

Statistical analysis was performed with a statistics package—Statistica 6.0 software (Statsoft; Cracow, Poland) using one way ANOVA followed by post tests for selected pairs of data and regression analysis. Results were expressed as mean of 5–10 assays ± S.D. For equilibrium binding data non-linear regression Origin 6.1 software was used and the goodness of fit of the predicted value from different equations to the data set obtained from three independent experiments was determined by χ^2 analysis. *P*-values <0.05 were considered statistically significant.

2. Results

Table 1 and Fig. 1 depict the cell cycle changes in C34 and E47 cells in the presence of APAP (5 mM; 48 h), BSO (pretreatment for 24 h with 100 μM BSO, prior to APAP) or MP (5 mM; 24 h). In C34 cells (Fig. 1, histograms A-F), APAP treatment was without any significant effect on cell cycle (histogram A, control C34 cells; histogram D, C34 cells treated with APAP) but notable alterations in cell cycle progression were seen in C34 cells pretreated with BSO and treated with APAP (histogram E). In BSO-pretreated C34 cells, APAP increased damaged, early G0/G1 cell numbers, from about 1% (histogram A) to 14% of cells (histogram C). S-phase cells also increased from about 14% (histogram A) to 29% (histogram C) while G2/M cell numbers declined from 13% to about 2%. BSO alone was without significant effect on cell cycle in C34 and E47 cells, although slower cell cycle progression could be noticed (histograms B and H). In E47 cells APAP increased hypodiploid cell numbers (histogram G versus histogram J) from 6 to 42% of total cell numbers ($P < 0.001$) and blocked cell division (more than two-fold increase in S-phase cell numbers; histogram G versus histogram J; $P < 0.01$). In BSO-pretreated E47 cells (histogram K) cytotoxicity of APAP was higher ($P < 0.01$) than in E47

Table 1
Effect of acetaminophen on cell cycle profiles in HepG2 cells (C34) and HepG2 cells overexpressing CYP2E1 (E47)

		A control	B BSO	C 4-MP	D APAP	E APAP + BSO	F APAP + MP
(I) EarlyG0/G1	C34	1.2 ± 0.8	3.5 ± 1.1	4.4 ± 2.1	7.4 ± 2.1	15.9 ± 5.7	14.4 ± 4.5
	E47	4.1 ± 1.2	5.3 ± 2.1	4.3 ± 2.2	42.4 ± 7.3	65.7 ± 11.5	21.1 ± 4.9
(II) G0/G1	C34	73.1 ± 5.5	71.2 ± 8.6	75.1 ± 8.3	71.5 ± 4.9	70.3 ± 7.2	68.9 ± 6.8
	E47	74.5 ± 5.8	73.4 ± 9.2	72.8 ± 5.8	67.6 ± 4.8	58.1 ± 9.2	65.8 ± 7.8
(III) S	C34	13.5 ± 4.5	16.4 ± 4.8	14.3 ± 5.2	19.1 ± 4.2	27.3 ± 6.2	17.0 ± 4.1
	E47	12.5 ± 3.9	17.9 ± 4.6	14.7 ± 4.8	27.4 ± 7.3	38.8 ± 6.7	23.3 ± 6.2
(IV) G2/M	C34	13,4 ± 3.1	12.4 ± 4.1	10,6 ± 3.3	9.4 ± 3.6	2.4 ± 2.1	14.1 ± 3.7
	E47	13.0 ± 2.7	8.7 ± 3.7	12,5 ± 3.8	5.0 ± 3.8	3.1 ± 2.2	10.9 ± 3.8

Chosen statistically significant differences between selected pairs of data in: early G0/G1 cell numbers (C34 cells)—AE***, AF***, BE**, CF**, DE*, DF*; (E47 cells)—AD***, AE***, AF*, BE***, CF*, DE**, DF**; in S-phase cell numbers (C34 cells)—AE*; E47—AD*, AE***, BE**; in G2/M cell numbers (C34 cells)—AE**, BE **; (E47 cells)—AE*. Other statistically significant differences were found in early G0/G1 cell numbers of C34 and E47 cells in group D (***) and E (***), and in S-phase cell numbers in group D (**). (*) $P < 0.05$; (**) $P < 0.01$; and (***) $P < 0.001$; $n = 5$.

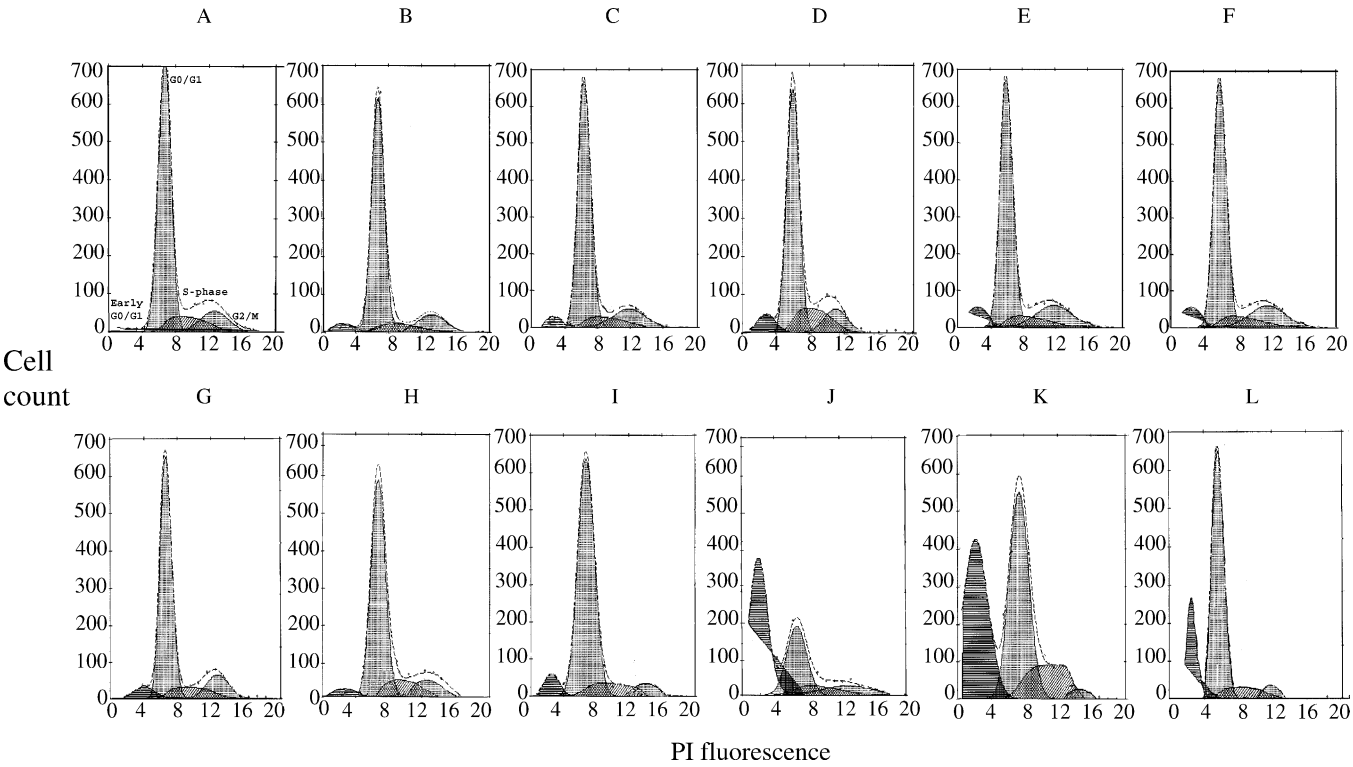

Fig. 1. The human hepatoblastoma cell subline-HepG2 (C34) and HepG2 cells stably transfected with human CYP2E1 (E47 cells) were treated with 5 mM acetaminophen (APAP) for 48 h. The drug cytotoxicity was determined by flow cytometry estimation of the cellular DNA ploidy using propidium iodide (PI) staining. The cells were quantified by their relative distribution in the hypodiploid (early GO/G1 zone of the DNA fluorescence histograms), diploid (G0/G1 zone—pre-DNA synthesis/resting), S-phase (DNA synthesis), and G2/M (post-DNA synthesis/mitosis) phases of the cell cycle (shown in histogram A).

cells treated with APAP alone (histogram G) or BSO alone (histogram H; $P < 0.001$), while cell cycle progression was lower (two-fold increase in S-phase cell numbers ($P < 0.01$) and decreased G2/M cell numbers; histogram E) than in APAP-treated cells; histogram J). These results are detailed in Table 1.

Intracellular Ca^{2+} levels in control and APAP-treated cells are shown in Fig. 2. APAP induced almost two-fold

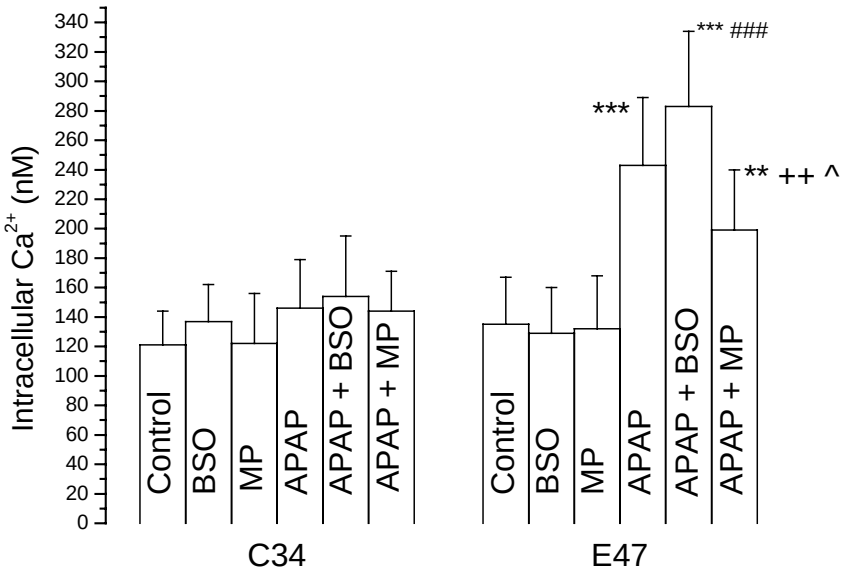

Fig. 2. Intracellular Ca^{2+} levels in HepG2 cells (C34) and HepG2 cells transfected with human CYP2E1 (E47 cells) treated with 5 mM acetaminophen (APAP) for 48 h. Each bar is a mean of 6 assays ± S.D. Statistically significant differences were found in E47 cells, between control and APAP-treated cells $^{***}(P < 0.001)$, control and APAP + BSO-treated cells $^{***}(P < 0.001)$, control and APAP + MP-treated cells $^{**}(P < 0,01)$; between cells treated with BSO and APAP + BSO ((###)$P < 0.001$); between MP and APAP + MP-treated E47 cells ((++)$P < 0.01$) and between APAP and APAP + MP-treated cells ((^)$P < 0.05$).

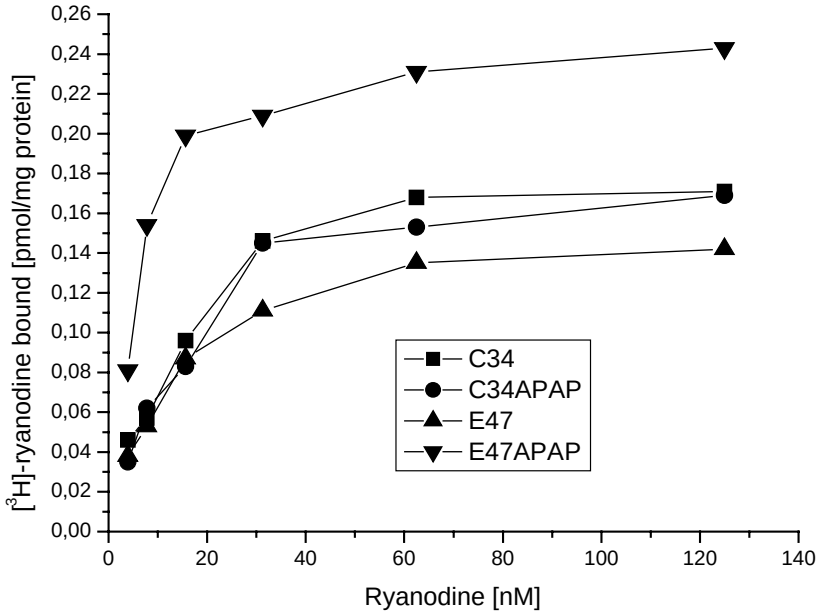

Fig. 3. Saturation plots of [^{3}H]ryanodine binding to microsomal fractions isolated from HepG2 cells (C34) and HepG2 cells overexpressing CYP2E1 (E47). C34 cells (■), C34 cells treated for 48 h with 5 mM acetaminophen (●), E47 cells (▲) and E47 cells treated with 5 mM acetaminophen for 48 h (▼).

Table 2
The effect of APAP on [^{3}H]ryanodine binding to microsomal fraction isolated from HepG2 cells (C34) and HepG2 cells overexpressing CYP2E1 (E47)

	Control		APAP	
	B_{max}	k_d	B_{max}	k_d
C34 cells	0.202	15.6	0.196	16.9
E47 cells	0.160	13.9	0.263	7.6

Values were determined using nonlinear regression (Origin 6.1) of the data shown in Fig. 2.

increase of the intracellular Ca^{2+} in E47 and even stronger increase in cells pretreated with BSO. Such effect was not observed in C34 cells. [Ca^{2+}] increase in E47 cells was significantly, but not completely inhibited by MP, indicating that the CYP2E1-dependent metabolism of APAP affects the intracellular calcium homeostasis.

Fig. 3 and Table 2 show [^{3}H]ryanodine binding to RyR in microsomal fractions isolated from C34 or E47 cells treated with APAP. There was no significant difference in $\equiv_{max}$ and k_d of the ligand in both cell types, but in E47 cells, APAP treatment increased both maximal ryanodine binding (64% increase) and ligand affinity (45% increase).

Plots of [^{3}H]ryanodine binding to microsomal fractions isolated from E47 cells as a function of incubation time and their linear transformations are shown in Fig. 4 A and B. APAP treatment increased association rate of the ligand (increased association rate constant by 72%; A, $P < 0.05$) without affecting ligand dissociation (B). Kinetic parameters are detailed in Table 3.

Fig. 5 shows Ca^{2+} fluxes in microsomal fractions obtained from control (plot 1), BSO-treated (plot 2), APAP-treated (plot 3) and APAP and BSO-treated E47 cells (plot 4). Each plot is a mean of 6–8 Ca^{2+} load assays ± S.D. No significant alterations in Ca^{2+} dynamics were observed in assays with microsomes isolated from C34 cells (results not shown), while microsomes isolated from APAP-treated E47 cells (trace 3) and from cells treated with APAP and pretreated with BSO (trace 4) had significantly slower initial Ca^{2+} loads. Initial Ca^{2+} pumping velocity in APAP-treated cells was decreased by about 53% ($P < 0.05$) while BSO pretreatment with subsequent APAP treatment resulted in significant (92%; $P < 0.01$) reduction of net Ca^{2+} uptake comparing to control. When cells were treated with BSO only, there were no alterations in initial (up to sixth min) Ca^{2+} uptake/release dynamics. However, it should be noted, that Ca^{2+} uptake by microsomes isolated from control or BSO-treated cells was curvilinear and significantly slower in late phases of the experiment (6–10 min) than in initial 6 min by 83 and 67%, respectively. Thus, the net Ca^{2+} uptake by microsomes isolated from E47 cells treated

Table 3
The effect of APAP on kinetics of [^{3}H]ryanodine association and dissociation to microsomal fraction isolated from cells overexpressing CYP2E1 (E47)

	k_{obs} (min^{-1})	$t_{1/2}$ (min)	k_{off} (min^{-1})	k_{on} (min^{-1}/nM^{-1})	k_d (k_{off}/k_{on})
Control E47 cells	0.00954	72.6	0.00389	0.000259	15.0
E47 cells +APAP	0.01639	42.3	0.00396	0.000829	4.77

Values were determined using non-linear regression (Origin 6.1) of the data shown in Fig. 4A and B.

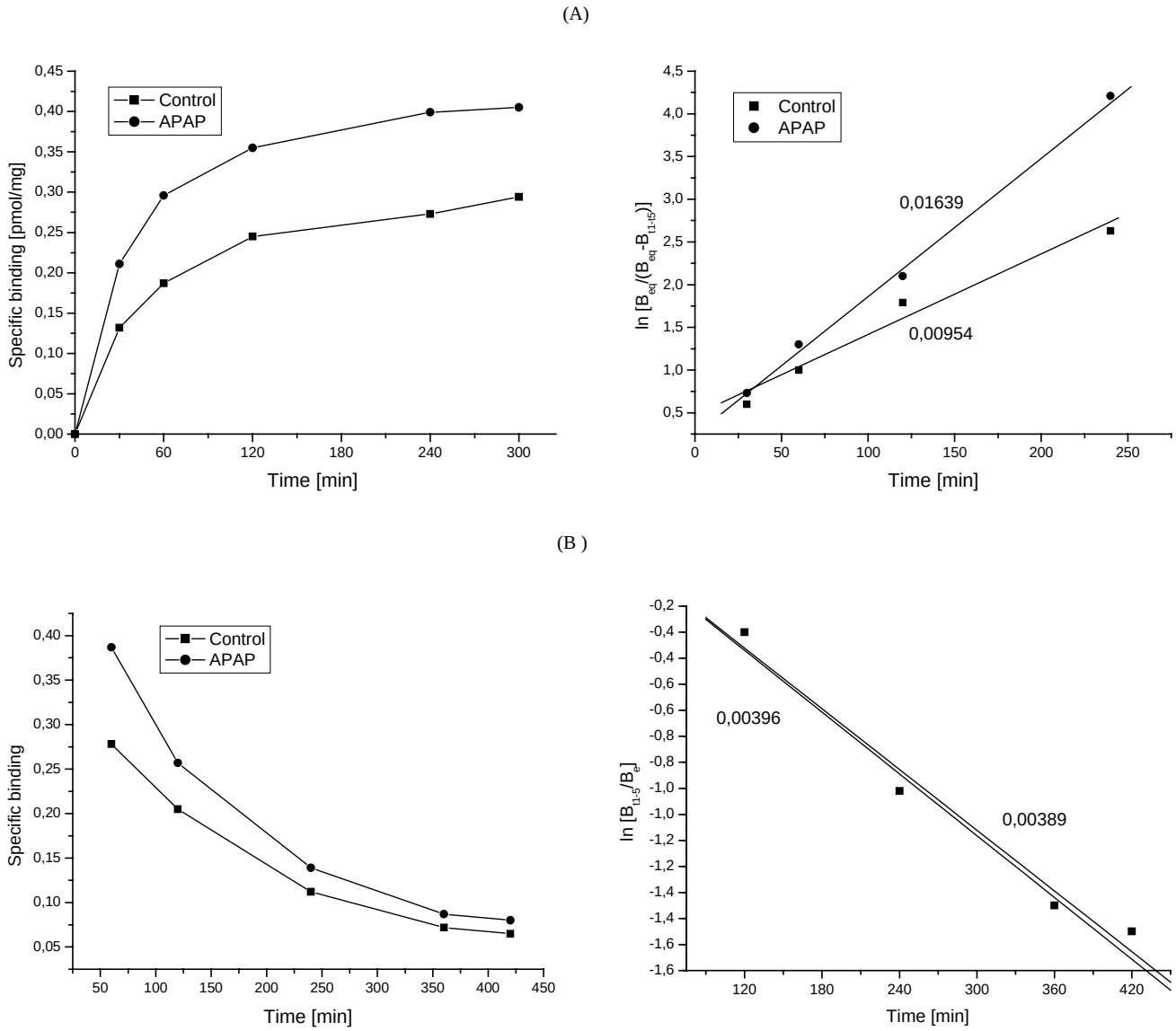

Fig. 4. [^{3}H]ryanodine (A) association and (B) dissociation kinetics in microsomal fractions isolated from control and APAP-treated HepG2 overexpressing CYP2E1 (E47) and their linear transformations. Data were analyzed by nonlinear regression (Origin 6.1).

with APAP measured over 10 min of pumping experiments was not significantly different from control (trace 1 versus trace 3) or BSO-treated cells (trace 2 versus trace 3).

Ca^{2+}/Mg^{2+}-ATPase activity was similar in all microsomal fractions (results not shown).

3. Discussion

CYP2E1 is the minor P450 isozyme in human liver and metabolizes relatively few drugs [27], but it is well documented that the most popular analgesic—APAP undergoes a CYP2E1-mediated metabolism to reactive quinones, which can arylate liver protein thiols and induce necrotic changes [2,28,29]. APAP may increase cytosolic calcium levels [13,30–32], however, the mechanism is not well understood. NAPQI and its metabolites may release Ca^{2+} from isolated liver microsomes and modulate microsomal ryanodine binding [16]. Ryanodine is a plant alkaloid that is known to specifically interact with the active, open state of the calcium-gated calcium-releasing channel—RyR [33], thus, the rate of occupancy of RyR by the ligand may serve as a measure of functional alterations of the channel. In contrast to the cardiac and skeletal isoforms of the RyR, the hepatic ryanodine-sensitive calcium channel is not well characterized, even if molecular and functional evidence of liver RyRs expression is well known. Hepatic endoplasmic reticulum contains calcium stores that are sensitive to ryanodine [34–38] but neither caffeine nor free Ca^{2+} (potent activators of cardiac and skeletal RyRs) can release Ca^{2+} from hepatic microsomes [33,36]. On the other hand, Ca^{2+} can be released from liver microsomes by quinones [39,40], thiol reagents [18,41] or reactive disulfides [19]. The early

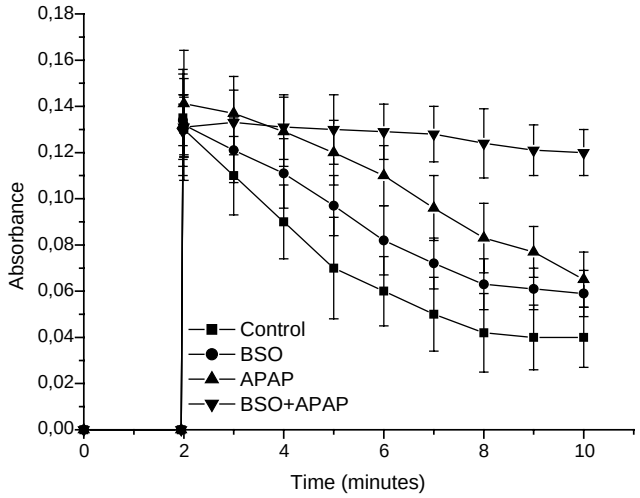

Fig. 5. Time courses of calcium uptake by microsomes isolated from: control (1), BSO-treated (2), APAP-treated (3) and APAP and BSO-treated HepG2 cells overexpressing CYP2E1 (E47). Ca^{2+} uptake was linear in each sample up to about 6th min of the experiment when some decrease in pumping efficiency was observed in microsomes isolated from control (trace 1) and BSO-treated (trace 2) cells. BSO treatment was without effect on the initial (up to 6th min) Ca^{2+} uptake/release dynamics ($P > 0.05$) while microsomes isolated from APAP-treated E47 cells (trace 3) had significantly slower (by 53%) initial pumping rates. In E47 cells pretreated with BSO and treated with APAP (trace 4) Ca^{2+} uptake was decreased by 92% comparing to control E47 cells.

stage of oxidative modification of the RyRs is characterized by an increased ryanodine binding to the microsomal membranes, a change that reflects the activation (opening) of the calcium channel; upon further thiol alteration, the ability of the calcium channel to bind ryanodine declines [39].

In the present study, we attempted to find out if CYP2E1-dependent metabolism of APAP influences intracellular Ca^{2+} homeostasis in hepatoblastoma cells. The comparison of APAP metabolism by HepG2 and E47 cells confirmed that CYP2E1 is required to induce cytotoxicity. At toxicologically relevant concentrations, 2 days of treatment with APAP caused the death of about 42% of the E47-cell population, with only little effect on non-transfected HepG2 cells. APAP itself seems to have some anti-proliferative effect, and this observation is in agreement with the previous data [6,11,42].

We have observed more than two-fold increase of $[Ca^{2+}]_i$ in Fura-2AM-stained, APAP-treated E47 cells. Such increase could reflect an increased accumulation of extracellular Ca^{2+}, and/or release of Ca^{2+} from intracellular calcium stores. In previous experiments with pheochromocytoma cells engineered to overexpress CYP2E1, we could not prevent the APAP-induced increase of $[Ca^{2+}]_i$ via chelation of the extracellular calcium with EGTA; plasma membrane Ca^{2+} channel blockers also had a very limited protective effect [43–45]. Alternatively, APAP-derived quinones may affect the intracellular, microsomal Ca^{2+} stores [16,39]. It is interesting to speculate that this mechanism may operate in intact cells as the CYP450 enzymatic system in hepatocytes is largely localized in the microsomal membranes and CYP450-derived APAP metabolites may preferentially react with neighboring proteins such as those that regulate the microsomal calcium homeostasis. With regard to the integrity of the microsomal calcium stores in intact cells, two pools of NAPQI could be considered as produced during the metabolism of APAP, on the cytosolic surface, which correspond to the localization of the active sites of CYP2E1, and on the intralumenal surface, where CYP3A4 may be localized [11].

The microsomal Ca^{2+} levels are co-regulated by Ca^{2+}/Mg^{2+}-ATPase that transports Ca^{2+} from the cytosol into the ER, Ca^{2+}-binding proteins, inositol-1,4,5-trisphosphate and/or ryanodine receptors that release Ca^{2+} back to the cytosol and other less known mechanisms. The Ca^{2+}/Mg^{2+}-ATPase and both the inositol-1,4,5-trisphosphate and ryanodine receptors are thiol-containing proteins whose functions depend on the red-ox status of their thiol groups [19,46,47]. A selective modification of the ryanodine-binding protein(s), as compared to other thiol-containing proteins (e.g. the Ca^{2+}/Mg^{2+}-ATPase), could be envisaged if its thiol groups had relatively lower pK_a values [48].

APAP treatment increased maximal ryanodine binding by 64% and elevated ligand affinity by 45% in E47 cells. This was probably due to increased association of the ligand (increased association rate constant by about 72%) since no change in ligand dissociation was observed. Ca^{2+} load experiments indicated reduced net Ca^{2+} uptake in microsomes isolated from E47 cells treated with APAP and significantly stronger block of Ca^{2+} load in microsomal fractions obtained from glutathione depleted E47 treated with APAP. Since Ca^{2+}/Mg^{2+}-ATPase activity was unaffected our results most probably reflect modification of RyRs by APAP metabolites or functional alteration in RyR thiols. This may suggest that Ca^{2+} release from the ryanodine-sensitive calcium channel may be important target for certain toxins like for example compounds activated by CYP45O located in the same cellular compartment to increase intracellular Ca^{2+} levels. However precise role of the hepatic, ryanodine-sensitive calcium channel in drug toxicity merits systematic studies.

Acknowledgments

These studies were supported by Grant 6PO5A 04020 from KBN.

References

[1] Hardman JG. Goodman Gilman's The Pharmacological Basis of Therapeutics. New York: Pergamon Press; 2001.
[2] Patten CJ, Thomas PE, Guy RL, Lee M, Gonzalez FJ, Guengerich FP, et al. Cytochrome P450 enzymes involved in acetaminophen

activation by rat and human liver microsomes and their kinetics. Chem Res Toxicol 1993;6:511–8.
[3] Thummel KE, Lee CA, Kunze KL, Nelson SD, Slattery JT. Oxidation of acetaminophen to *N*-acetyl-*p*-aminobenzoquinone imine by human CYP3A4. Biochem Pharmacol 1993;45:1563–9.
[4] Tonge RP, Kelly EJ, Bruschi SA, Kalhorn T, Eaton DL, Nebert DW, et al. Role of CYP1A2 in the hepatotoxicity of acetaminophen: investigations using Cyp1a2 null mice. Toxicol Appl Pharmacol 1998;153:102–8.
[5] Lee CA, Lillibridge JH, Nelson SD, Slattery JT. Effects of caffeine and theophylline on acetaminophen pharmacokinetics: P450 inhibition and activation. J Pharmacol Exp Ther 1996;277:287–91.
[6] Dai Y, Cederbaum AI. Cytotoxicity of acetaminophen in human cytochrome P4502E1-transfected HepG2 cells. J Pharmacol Exp Ther 1995;273:1497–505.
[7] Cohen SD, Pumford NR, Khairallah EA, Boekelheide K, Pohl LR, Amouzadeh HR, et al. Selective protein covalent binding and target organ toxicity. Toxicol Appl Pharmacol 1997;143:1–12.
[8] Pumford NR, Halmes NC. Protein targets of xenobiotic reactive intermediates. Annu Rev Pharmacol Toxicol 1997;37:91–117.
[9] Chen W, Koenigs LL, Thompson SJ, Peter RM, Rettie AE, Trager WF, et al. Oxidation of acetaminophen to its toxic quinone imine and nontoxic catechol metabolites by baculovirus-expressed and purified human cytochromes P450 2E1 and 2A6. Chem Res Toxicol 1998;11: 295–301.
[10] Chen W, Shockcor JP, Tonge R, Hunter A, Gartner C, Nelson SD. Protein and nonprotein cysteinyl thiol modification by *N*-acetyl-*p*-benzoquinone imine via a novel ipso adduct. Biochemistry 1999;38: 8159–66.
[11] Zhou L, Erickson RR, Holtzman JL. Studies comparing the kinetics of cysteine conjugation and protein binding of acetaminophen by hepatic microsomes from male mice. Biochim Biophys Acta 1997;1335:153–60.
[12] Moore M, Thor H, Moore G, Nelson S, Moldeus P, Orrenius S. The toxicity of acetaminophen and *N*-acetyl-*p*-benzoquinone imine in isolated hepatocytes is associated with thiol depletion and increased cytosolic Ca^{2+}. J Biol Chem 1985;260:13035–40.
[13] Shen W, Kamendulis LM, Ray SD, Corcoran GB. Acetaminophen-induced cytotoxicity in cultured mouse hepatocytes: correlation of nuclear Ca^{2+} accumulation and early DNA fragmentation with cell death. Toxicol Appl Pharmacol 1991;111:242–54.
[14] Satorres J, Perez-Mateo M, Mayol MJ, Esteban A, Graells ML. Protective effect of diltiazem against acetaminophen hepatotoxicity in mice. Liver 1995;15:16–9.
[15] Weis M, Moore GA, Cotgreave IA, Nelson SD, Moldeus P. Quinone imine-induced Ca^{2+} release from isolated rat liver mitochondria. Chem Biol Interact 1990;76:227–40.
[16] Stoyanovsky DA, Cederbaum AI. Metabolites of acetaminophen trigger Ca^{2+} release from liver microsomes. Toxicol Lett 1999;106: 23–9.
[17] Stoyanovsky D, Murphy T, Anno PR, Kim YM, Salama G. Nitric oxide activates skeletal and cardiac ryanodine receptors. Cell Calcium 1997;21:19–29.
[18] Xu L, Eu JP, Meissner G, Stamler JS. Activation of the cardiac calcium release channel (ryanodine receptor) by poly-*S*-nitrosylation. Science 1998;279:234–7.
[19] Zaidi NF, Lagenaur CF, Abramson JJ, Pessah I, Salama G. Reactive disulfides trigger Ca^{2+} release from sarcoplasmic reticulum via an oxidation reaction. J Biol Chem 1989;264:21725–36.
[20] Mari M, Bai J, Cederbaum AI. Toxicity by pyruvate in HepG2 cells depleted of glutathione: role of mitochondria. Free Radic Biol Med 2002;32:73–83.
[21] Morasca L, Erba E. Animal Cell Culture, A Practical Approach. Oxford: IRL Press; 1986.
[22] Grynkiewicz G, Poenie M, Tsien RY. A new generation of Ca^{2+} indicators with greatly improved fluorescence properties. J Biol Chem 1985;260:3440–50.
[23] Tsien R, Pozzan T. Measurement of cytosolic free Ca^{2+} with quin2. Methods Enzymol 1989;172:230–62.
[24] Palakodety RB, Clejan LA, Krikun G, Feierman DE, Cederbaum AI. Characterization and identification of a pyrazole-inducible form of cytochrome P-450. J Biol Chem 1988;263:878–84.
[25] Srivastava SP, Chen NQ, Holtzman JL. The in vitro NADPH-dependent inhibition by CCl4 of the ATP-dependent calcium uptake of hepatic microsomes from male rats. Studies on the mechanism of the inactivation of the hepatic microsomal calcium pump by the $CCl_3^{\bullet}$ radical. J Biol Chem 1990;265:8392–9.
[26] Martinez-Merlos T, Canedo-Merino R, Diaz-Munoz M. Ryanodine receptor binding constants in skeletal muscle, heart. Int J Biochem Cell Biol 1997;29:529–39.
[27] Caro AA, Cederbaum AI. Oxidative stress, toxicology, and pharmacology of cyp2e1. Annu Rev Pharmacol Toxicol 2004;44:27–42.
[28] Matthews AM, Roberts DW, Hinson JA, Pumford NR. Acetaminophen-induced hepatotoxicity. Analysis of total covalent binding vs. specific binding to cysteine. Drug Metab Dispos 1996;24:1192–6.
[29] Jaeschke H, Gores GJ, Cederbaum AI, Hinson JA, Pessayre D, Lemasters JJ. Mechanisms of hepatotoxicity. Toxicol Sci 2002; 65:166–76.
[30] Davies DS, Fawthrop DJ, Nasseri-Sina P, Wilson JW, Hardwick SJ, Boobis AR. Paracetamol toxicity and its prevention by cytoprotection with iloprost. Toxicol Lett 1992;64-65:575–80.
[31] Holownia A, Mapoles J, Menez JF, Braszko JJ. Acetaminophen metabolism and cytotoxicity in PC12 cells transfected with cytochrome P4502E1. J Mol Med 1997;75:522–7.
[32] Thibault N, Peytavin G, Claude JR. Calcium channel blocking agents protect against acetaminophen-induced cytotoxicity in rat hepatocytes. J Biochem Toxicol 1991;6:237–8.
[33] el-Hayek R, Lokuta AJ, Arevalo C, Valdivia HH. Peptide probe of ryanodine receptor function. Imperatoxin A, a peptide from the venom of the scorpion *Pandinus imperator*, selectively activates skeletal-type ryanodine receptor isoforms. J Biol Chem 1995;270: 28696–704.
[34] Shoshan-Barmatz V, Zhang GH, Garretson L, Kraus-Friedmann N. Distinct ryanodine- and inositol 1,4,5-trisphosphate-binding sites in hepatic microsomes. Biochem J 1990;268:699–705.
[35] Shoshan-Barmatz V, Pressley TA, Higham S, Kraus-Friedmann N. Characterization of high-affinity ryanodine-binding sites of rat liver endoplasmic reticulum. Differences between liver and skeletal muscle. Biochem J 1991;276:41–6.
[36] Lilly LB, Gollan JL. Ryanodine-induced calcium release from hepatic microsomes and permeabilized hepatocytes. Am J Physiol 1995;268: G1017–24.
[37] Feng L, Pereira B, Kraus-Friedmann N. Different localization of inositol 1,4,5-trisphosphate and ryanodine binding sites in rat liver. Cell Calcium 1992;13(2):79–87.
[38] Lee BS, Sessanna S, Laychock SG, Rubin RP. Expression and cellular localization of a modified type 1 ryanodine receptor and L-type channel proteins in non-muscle cells. J Membr Biol 2002;189:181–90.
[39] Feng W, Liu G, Xia R, Abramson JJ, Pessah IN. Site-selective modification of hyperreactive cysteines of ryanodine receptor complex by quinones. Mol Pharmacol 1999;55:821–31.
[40] Liu G, Abramson JJ, Zable AC, Pessah IN. Direct evidence for the existence and functional role of hyperreactive sulfhydryls on the ryanodine receptor-triadin complex selectively labeled by the coumarin maleimide 7-diethylamino-3-(4′-maleimidylphenyl)-4-methylcoumarin. Mol Pharmacol 1994;45:189–200.
[41] Zable AC, Favero TG, Abramson JJ. Glutathione modulates ryanodine receptor from skeletal muscle sarcoplasmic reticulum. Evidence for redox regulation of the Ca^{2+} release mechanism. J Biol Chem 1997;272:7069–77.
[42] Mapoles J, Berthou F, Alexander A, Simon F, Menez JF. Mammalian PC-12 cell genetically engineered for human cytochrome P450 2E1 expression. Eur J Biochem 1993;214:735–45.

[43] Ray SD, Kamendulis LM, Gurule MW, Yorkin RD, Corcoran GB. Ca^{2+} antagonists inhibit DNA fragmentation and toxic cell death induced by acetaminophen. FASEB J 1993;7:453–63.
[44] Dimova S, Koleva M, Rangelova D, Stoythchev T. Effect of nifedipine, verapamil, diltiazem and trifluoperazine on acetaminophen toxicity in mice. Arch Toxicol 1995;70:112–28.
[45] Holownia A, Menez JF, Braszko JJ. The role of calcium in paracetamol (acetaminophen) cytotoxicity in PC12 cells transfected with CYP4502E1. Inflammopharmacology 1998;6:133–42.
[46] Porter Moore C, Zhang JZ, Hamilton SL. A role for cysteine 3635 of RYR1 in redox modulation and calmodulin binding. J Biol Chem 1999;274:36831–4.
[47] Haarmann CS, Fink RH, Dulhunty AF. Oxidation and reduction of pig skeletal muscle ryanodine receptors. Biophys J 1999;77:3010–22.
[48] Pessah IN, Beltzner C, Burchiel SW, Sridhar G, Penning T, Feng W. A bioactive metabolite of benzo[*a*]pyrene, benzo[*a*]pyrene-7,8-dione, selectively alters microsomal Ca^{2+} transport and ryanodine receptor function. Mol Pharmacol 2001;59:506–13.